Polymer 49 (2008) 2170–2175

Contents lists available at ScienceDirect

Polymer

journal homepage: www.elsevier.com/locate/polymer

Property of diblock copolymer having extremely narrow molecular weight distribution

Soojin Park [a], Du Yeol Ryu [b,1], Jin Kon Kim [b], Moonhor Ree [a], Taihyun Chang [a,*]

[a] Department of Chemistry, Polymer Research Institute, Pohang University of Science and Technology, San 31, Hyoja-Dong, Nam-Gu, Pohang 790-784, Republic of Korea
[b] Department of Chemical Engineering, Polymer Research Institute, Pohang University of Science and Technology, San 31, Hyoja-Dong, Nam-Gu, Pohang 790-784, Republic of Korea

ARTICLE INFO

Article history:
Received 20 January 2008
Received in revised form 2 March 2008
Accepted 4 March 2008
Available online 8 March 2008

Keywords:
Polystyrene-*block*-polyisoprene
HPLC fractionation
Microphase

ABSTRACT

Molecular weight distribution effect on the morphological behavior of polystyrene-*block*-polyisoprene (PS-*b*-PI) diblock copolymers was investigated. PS-*b*-PI samples were prepared by anionic polymerization and further fractionated by HPLC to obtain the fractions of similar average molecular weight and composition but of narrower distributions in both molecular weight and composition. The strategy is to use reversed-phase LC to fractionate the PI block and normal phase LC to fractionate the PS block with a minimal effect on the other blocks. The interfacial thickness, grain size and the phase transition behavior of the unfractionated and fractionated PS-*b*-PI were compared by X-ray reflectivity, small angle X-ray scattering, transmission electron microscopy and rheological measurements. The fractionated PS-*b*-PI with more homogeneous molecular weight and composition exhibits a narrower interface, larger grain size and a sharper morphological transition compared to the unfractionated PS-*b*-PI.

1. Introduction

The ability of block copolymers to self-assemble into a variety of ordered structures with nano-scale periodicities has attracted considerable interest in fundamental aspects as well as various potential applications [1,2]. These structures of block copolymers can be controlled by varying the block composition or the incompatibility of the blocks [3–5] and have been explored recently to meet the demand for integrated circuits with smaller feature sizes, for photonic materials with periodic structures, for production of ultrahigh-density arrays of nanometer-scale elements [6–10].

The block copolymers are often prepared via anionic polymerization method. The anionic polymerization is the best available method to yield the polymers of the narrowest molecular weight distribution (MWD) [11] that are often regarded as "monodisperse" although the MWD of each block is far from the rigorous meaning of the term [12]. Various living radical polymerization methods are also able to produce block copolymers. They have a broader MWD than anionically polymerized samples but exhibit well-developed microdomain structures [13–15]. Nonetheless, the MW and composition distribution in the block copolymers must affect their self-assembled phase behavior. There are a few studies of the MWD effect on the phase behavior and these studies focused on the block copolymers of a broader MWD than the as-prepared polymers by anionic polymerization.

The MWD effects on the phase behavior of block copolymers have been investigated theoretically [16–18]. For example, the calculation of Sides and Fredrickson according to the self-consistent mean-field theory (SCFT) demonstrates a big influence of the MWD on the ordered phase behavior of diblock copolymers [16]. Cooke and Shi investigated the MWD effect on the phase diagram of diblock copolymers using SCFT. It was found that the order–disorder transition shifts to higher temperatures, as predicted by a random phase approximation analysis. For asymmetric polymer distributions, polydispersity favors structures with curved interfaces [17].

A few experimental studies were also carried out to investigate the effects of the MWD on diblock copolymer assembly [19–23]. Hashimoto et al. investigated the microdomain size distribution of polystyrene-*block*-polyisoprene (PS-*b*-PI) with a MWD larger ($M_w/M_n \sim 1.1$) than typical anionically polymerized sample [19]. They found that the uniformity of the microdomain size of the block copolymers was not affected significantly by MWD of block copolymers. Noro et al. investigated the MWD effect using blends of symmetric polystyrene-*block*-poly(2-vinylpyridine) (SP) and PSP triblock copolymers having the same composition but different MW. They observed that as MWD is widened, the lamellar domain spacing increased [20].

* Corresponding author. Tel.: +82 54 279 2109; fax: +82 54 279 3399.
E-mail address: tc@postech.ac.kr (T. Chang).
[1] Present address: Department of Chemical Engineering, Yonsei University, Seoul 120-749, Republic of Korea.

0032-3861/$ – see front matter © 2008 Elsevier Ltd. All rights reserved.
doi:10.1016/j.polymer.2008.03.009

We reported earlier that it is possible to fractionate the polymers prepared by anionic polymerization further into the polymers of narrower MWD by HPLC [24,25]. We have also shown that it is possible to fractionate the individual blocks of block copolymers to obtain block copolymers with narrower distribution in both MW and chemical composition [26–29]. Therefore, it is worthwhile to study what can be observed from the block copolymers with a narrower distribution than that of block copolymers as-prepared by anionic polymerization. In this study, three PS-*b*-PI diblock copolymers of different chemical compositions were prepared by anionic polymerization. These PS-*b*-PI samples were further fractionated by HPLC to obtain the block copolymers of narrower MWD for both blocks while maintaining the average MW and composition unchanged from the as-prepared or unfractionated block copolymer. The characteristics of phase-segregated morphology of these fractionated PS-*b*-PI samples were compared with that of the unfractionated samples. To our knowledge, this is the first experimental investigation of the MWD effect on the phase behavior of block copolymers with a narrower MWD than the block copolymers prepared by anionic polymerization.

2. Experimental section

2.1. Materials

PS-*b*-PI samples were prepared by sequential anionic polymerization at 45 °C under Ar atmosphere using *sec*-butyllithium (Aldrich) and cyclohexane (Aldrich) as an initiator and a solvent, respectively. After the polymerization of the styrene block was completed, isoprene monomer was added for the polymerization of the PI block. Details of the apparatus and the polymerization procedure were reported previously [30,31]. Three PS-*b*-PI samples of different volume fractions of PI block (f_{PI}) were used in this study (SI-1: $f_{PI} \approx 0.50$, SI-2: $f_{PI} \approx 0.38$, SI-3: $f_{PI} \approx 0.66$).

The PS-*b*-PI samples were fractionated by HPLC to obtain the polymers with narrower distribution in both molecular weight and composition (i.e., narrower MWD of individual blocks). The HPLC apparatus consists of a solvent delivery pump (Bischoff, 2250), a 10-port sample injector (Alltech, SelectPro) equipped with a 100 μL injection loop, and a variable wavelength UV/vis absorption detector (Spectra-Physics, SP8480) operated at a wavelength of 260 nm. For the reversed-phase (RP) LC fractionation, a C18 bonded silica column (Nucleosil, 100 Å pore, 70 × 22 mm ID) and a mixture of CH_2Cl_2/CH_3CN (80/20, v/v, Duksan, HPLC grade) were used as the stationary and the mobile phase, respectively. The sample concentration was 140 mg/mL and the flow rate of the mobile phase was 1.5 mL/min. Temperature of the column was kept at 20 °C. For the normal phase (NP) LC fractionation, a diol-bonded silica column (Nucleosil, 100 Å pore, 100 × 22 mm ID) and a mixture of isooctane/THF (75/25, v/v, Duksan, HPLC grade) as the stationary and the mobile phase, respectively. The sample concentration was 140 mg/mL and the flow rate of the mobile phase was 1.5 mL/min. The column temperature was kept at 15 °C.

For the size exclusion chromatography (SEC) analysis, two PL-gel columns (Polymer Lab., PL-mixed C, 300 × 7.5 mm ID) were used and the eluent was THF (Duksan, HPLC grade). The temperature of the column was kept at 40 °C using a column oven (Eppendorf, TC-50). Chromatograms were recorded with a multi-angle laser light scattering detector (MALLS, Wyatt, mini-DAWN) and a refractive index detector (Wyatt, Opti-Lab).

2.2. X-ray reflectivity (XR)

The specimens for all bulk measurements contain 0.3 wt% 2,6-di-*tert*-butyl-4-methylphenol (Aldrich) as an antioxidant. A 10 wt% polymer solution in toluene was spin-coated on a silicon wafer (30 × 10 mm) at 2000 rpm for 1 min. The samples were allowed to dry at room temperature for 3 h prior to the annealing at 120 °C for 24 h under vacuum. Then the samples were slowly cooled under vacuum to room temperature over a period of several hours. XR experiments were carried out using synchrotron radiation at the Pohang Light Source (PLS) [32]. The X-ray beam was monochromatized by a Si(111) double crystal monochromator to a wavelength (λ) of 0.154 nm and $\Delta\lambda/\lambda = 5 \times 10^{-4}$. The sample was mounted on a HUBER four-circle goniometer, and a scintillation counter with an enhanced dynamic range (Bede Scientific, EDR) was used to detect the reflected intensity during the $\theta - 2\theta$ scan.

2.3. Small angle X-ray scattering (SAXS)

The 10 wt% polymer/toluene solution containing the antioxidant was slowly dried at room temperature for 1 day and further dried under vacuum at 50 °C for 1 day. Then the polymer samples of 0.8 mm thickness were annealed at 120 °C for 24 h and slowly cooled under vacuum to room temperature over a period of several hours. SAXS measurements were carried out at the synchrotron SAXS facility in the PLS [33]. The wavelength (λ) of the X-ray beam was 1.608 Å and the energy resolution ($\Delta\lambda/\lambda$) was 1.5×10^{-2}. Beam size was smaller than 1 × 1 mm and the sample-to-detector distance was 160 cm. Scattering profiles were obtained at room temperature and at a heating rate of 2 °C/min and then corrected for absorption and air scattering.

2.4. Rheological measurement

A rheometer (Rheometrics, ARES) with parallel plates of 8 mm diameter was used to determine the dynamic storage and loss moduli (G' and G'') of PS-*b*-PI diblock copolymers from 90 to 220 °C at a heating rate of 1 °C/min under a nitrogen atmosphere. Strain amplitude (γ_o) and angular frequency are 0.05 and 0.1 rad/s, respectively, which lie in linear viscoelasticity.

2.5. Transmission electron micrographs (TEM)

Transmission electron micrographs were obtained to identify the morphology of the samples annealed at 120 °C for 24 h.

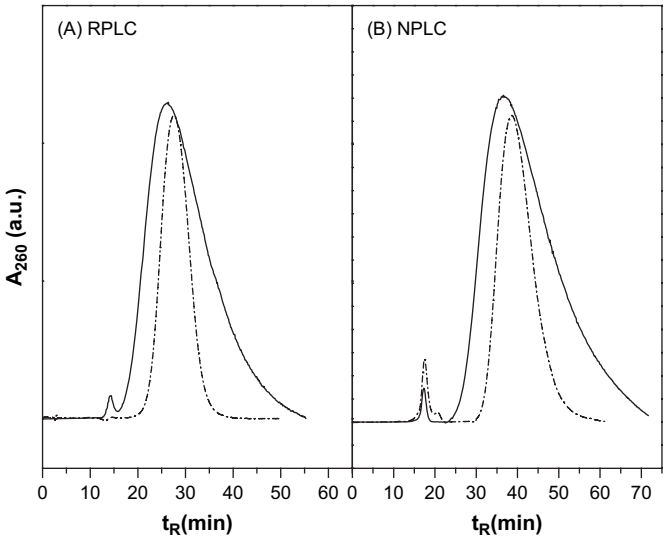

Fig. 1. Chromatograms of SI-1 before (solid line) and after (dashed line) the RPLC (A) and the subsequent NPLC (B) fractionation. RPLC fractionates the PI block of the diblock copolymer while NPLC fractionates the PS block. The HPLC fraction shows a much narrower distribution in both PS and PI blocks.

Table 1
Characteristics of unfractionated and fractionated PS-*b*-PI having similar molecular weight and composition

Samples[a]	M_n (kg/mol)[b]	M_w/M_n[b]	f_{PI}[c]
Unfractionated SI-1	23.1	1.04	0.500
Fractionated SI-1	23.0	1.01	0.500
Unfractionated SI-2	23.5	1.03	0.384
Fractionated SI-2	23.0	1.01	0.384
Unfractionated SI-3	34.0	1.03	0.665
Fractionated SI-3	32.7	1.01	0.657

[a] PS-*b*-PI samples were prepared by anionic polymerization and the homo-PS was removed by HPLC fractionation.
[b] Determined by SEC–light scattering detection.
[c] Volume fraction of the PI block determined by ^{1}H NMR spectroscopy.

Electron transparent films of the fractionated PS-*b*-PI were cryomicrotomed (RMC Ultracut) to a nominal thickness of 50–80 nm at −120 °C and transferred to Cu grids. The specimens were stained by exposure to OsO_4 (Polysciences, 0.4% in water) vapor for 30 min before taking bright-field TEM (Hitachi-7600) micrographs.

3. Results and discussion

3.1. HPLC fractionation

The detailed HPLC separation and characterization procedure were published elsewhere [26] and the separation principle is described briefly as follows. When a PS-*b*-PI is subjected to the RPLC separation, the retention of the diblock copolymer was determined mainly by the PI block length since the less polar PI block has a stronger affinity to the alkyl bonded stationary phase than the PS block. As shown in Fig. 1(A), the middle portion of the elution peak was collected to reduce the MWD of the PI block while keeping the average molecular weight of the PI block unaffected. On the other hand, the NPLC retention of PS-*b*-PI is mainly determined by the

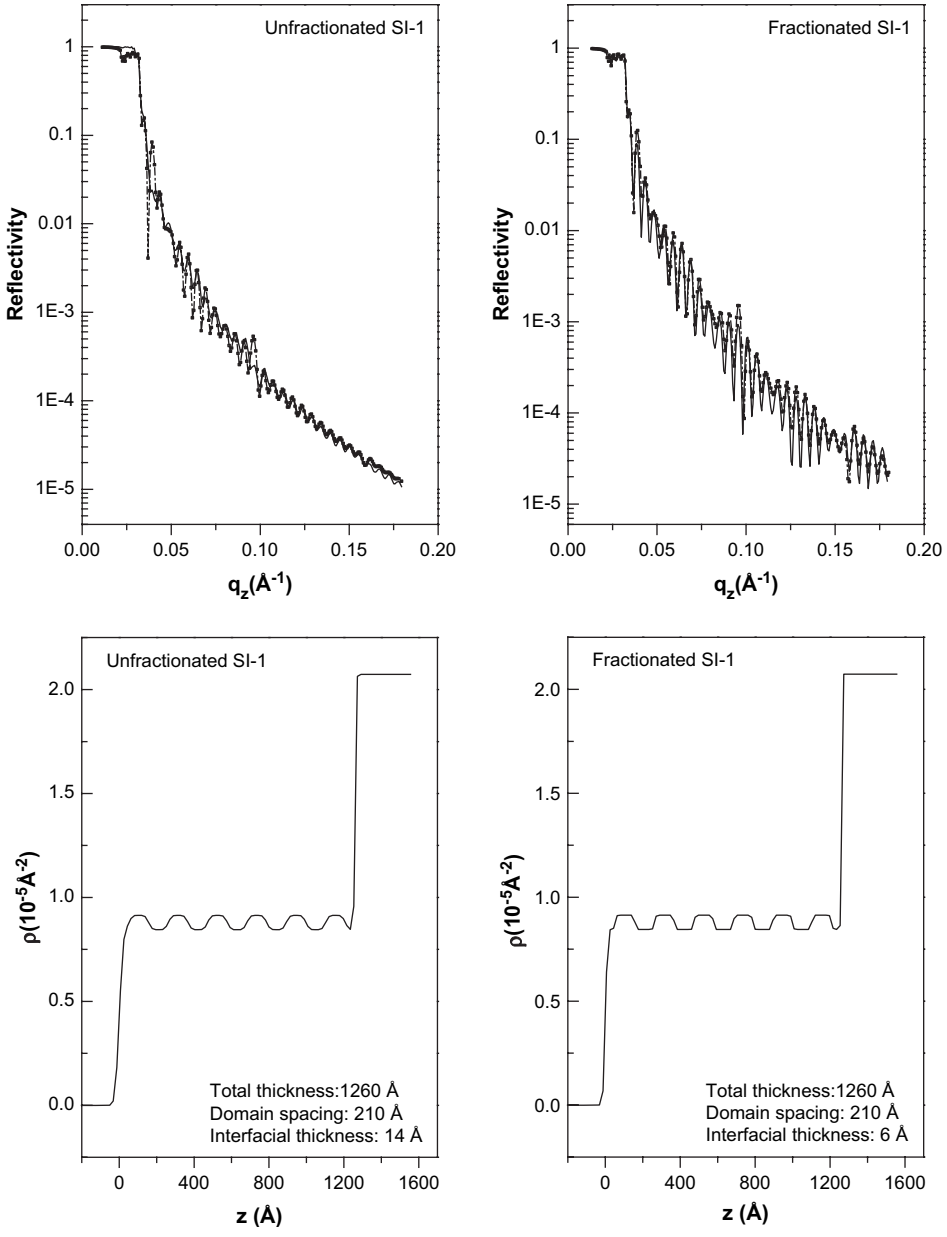

Fig. 2. X-ray reflectivity curve measured from thin PS-*b*-PI films (left: unfractionated SI-1, right: fractionated SI-1). The modulating Kiessig fringes of the fractionated sample are developed more clearly than the unfractionated copolymer. The filled squares and the solid line represent the experimental data and the fitted curve, respectively. The bottom plots show electron density profiles of the unfractionated PS-*b*-PI and fractionated samples obtained by fitting the X-ray reflectivity curve to the multi layer model of Parratt [36].

more polar PS block length. When the RPLC fraction was subjected to the NPLC separation, the elution peak is broad as shown in Fig. 1(B) since the RPLC fraction has a narrow distribution only in the PI block length. Again the middle portion of the elution peak was collected to reduce the MWD of the PS block, which completed the fractionation for both blocks.

As-prepared PS-*b*-PI samples contain small amount of homo-PS, inadvertently terminated PS precursors. The homo-PS is also removed in the fractionation process. The amount of homo-PS is small, less than 2 wt% in the as-prepared PS-*b*-PI. However, to investigate the difference in the phase behavior between the fractionated PS-*b*-PI and the unfractionated block copolymers solely due to the MWD, the homo-PS in the as-prepared PS-*b*-PI was also removed. In addition, the molecular weight and composition of the fractionated polymer match with the homo-PS free PS-*b*-PI slightly better than the as-prepared sample. The homo-PS removed PS-*b*-PI will be henceforth called as 'unfractionated' block copolymers. Molecular weight and composition of the block copolymers were determined by SEC and ^{1}H NMR spectroscopy (Bruker, DPX-300), respectively, and the results are summarized in Table 1. The volume fraction of PI block (f_{PI}) was calculated according to the following formula after Helfand [34]:

$$f_{PI} = (N_{PI}/\rho_{PI})/[(N_{PS}/\rho_{PS} + N_{PI}/\rho_{PI})] \quad (1)$$

where N_{PS} and N_{PI} are the number-average degree of polymerization of PS and PI blocks, and ρ_{PS} and ρ_{PI} are segmental densities of PS and PI, respectively, $\rho_{PS} = 1.01 \times 10^4$ mol/m^3 and $\rho_{PI} = 1.34 \times 10^4$ mol/m^3.

The fractionated samples obtained from the dual RPLC × NPLC fractionation process have a volume fraction and a molecular weight very similar to the unfractionated PS-*b*-PI but with much narrower MWD in both blocks as shown in Fig. 1. Unfortunately, however, we do not have a good mean to measure their MWD precisely. Although the difference between the fractionated PS-*b*-PI and unfractionated polymers is large enough to be detected by SEC coupled with light scattering detection, the M_w/M_n values determined by SEC for the polymer samples with such narrow MWD should not be precise due to the band broadening of SEC [12]. It is likely that the value of $M_w/M_n = 1.01$ represents the limit of SEC resolution due to the band broadening. Significantly lower M_w/M_n values are expected from the chromatograms in Fig. 1.

3.2. Interfacial thickness

Fig. 2 displays XR profiles of thin SI-1 films on a Si wafer. SI-1 has a symmetric composition and the lamellae of PS and PI domains are oriented parallel to the substrate plane. Once θ exceeds the critical angle of the substrate, a significant portion of the X-ray beam penetrates into the substrate and a sharp drop of the reflected intensity occurs. The steeply decaying reflectivity curve is modulated by Kiessig fringes [35]. These fringes appear due to the interference between the X-ray beams reflected from the film surface and

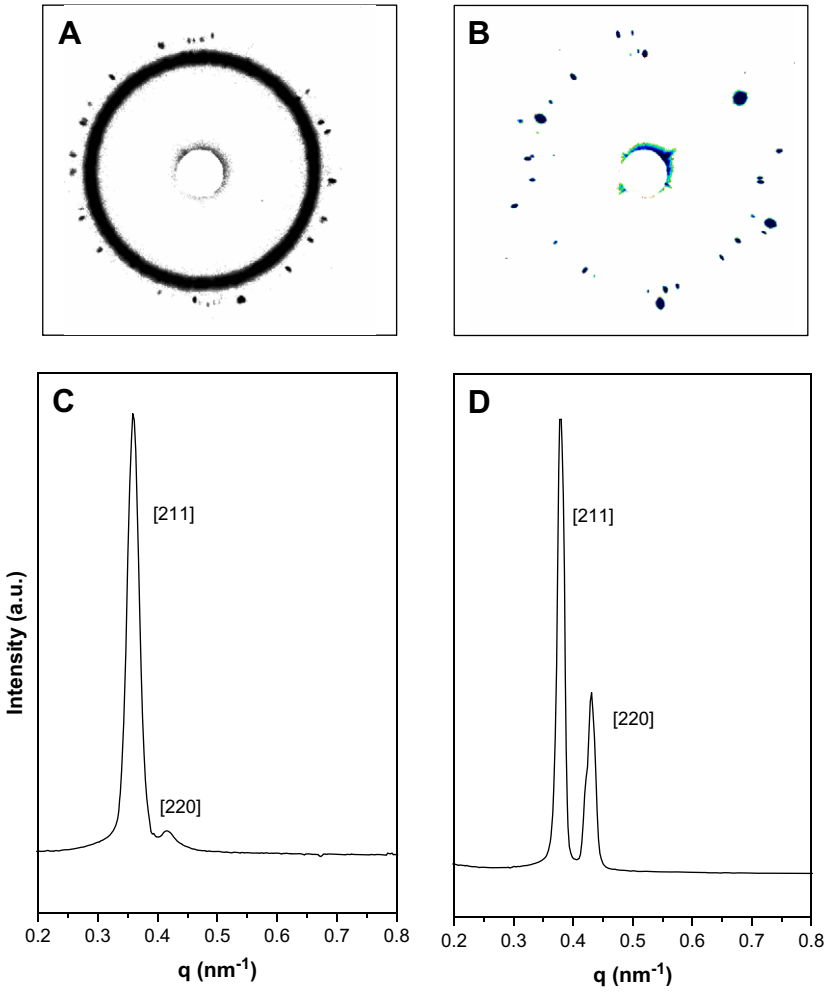

Fig. 3. 2D SAXS patterns and circular averaged scattering intensity profiles of unfractionated SI-2 (A, C) and the fractionated SI-2 (B, D). The fractionated sample shows strong diffraction spots from the both [211] and [220] planes. The circular average plots of (C) and (D) also show a clear difference between the two polymer samples that the diffraction peaks are much sharper and better developed in the fractionated sample. These results indicate that the fractionated sample has a long-range order.

from the film/substrate interface. Also the amplitude of Kiessig fringes is modulated at a lower frequency, which arises from the layer structure of the PS and PI domains. The modulating Kiessig fringes of the fractionated PS-*b*-PI show up much more clearly than the unfractionated PS-*b*-PI indicative of the sharper contrast in internal domain structure.

The film depth profile including the interfacial thickness can be estimated from the analysis of the XR curve. The XR data are fit with a nonlinear least squares algorithm using the recursive multilayer method of Parratt [36] and the fit parameters for PS, PI and Si wafer in the literature [37]. By fitting the XR profiles to the model, the internal structure of the thin films can be extracted. In the bottom plots of Fig. 2, the electron density profiles of PS-*b*-PI thin films are shown, from which we can note that the electron density profile in the fractionated sample shows a higher contrast than the unfractionated sample. While the total film thickness and the domain spacing are very similar at 1260 Å and at 210 Å for the both thin films, the interfacial thickness between the two block domains shows a clear difference: 14 Å for the unfractionated SI-1 and 6 Å for fractionated SI-1. It is clear that the homogeneity of the block copolymer leads to a better-developed internal structure of the phase-segregated morphology.

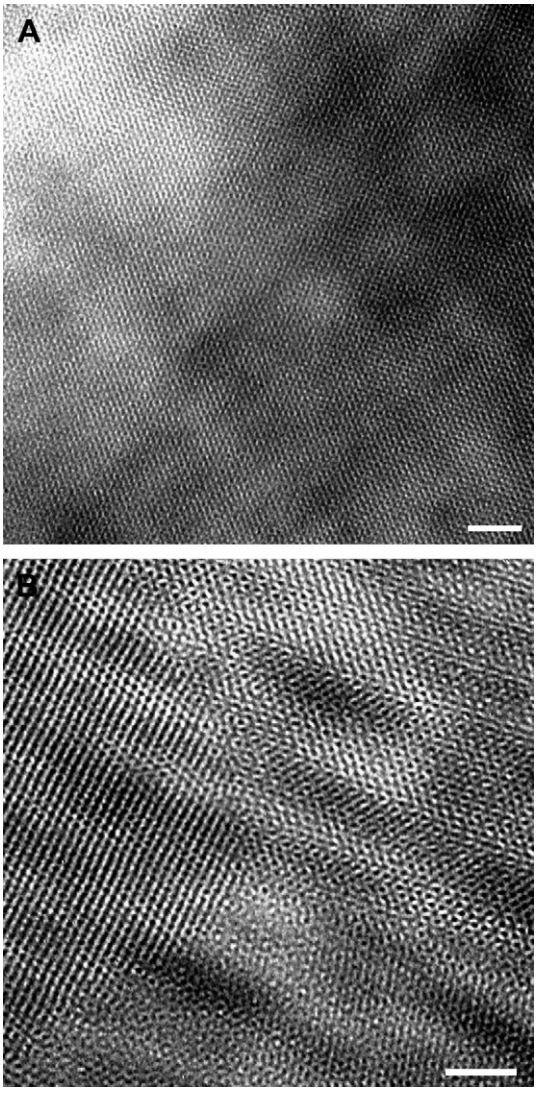

Fig. 4. TEM images of the fractionated (A) and unfractionated (B) SI-2 samples (scale bar: 100 nm). A single grain gyroid structure over the entire image is shown in fractionated sample, while a multi-grain structure is evident in unfractionated one.

3.3. Grain size

Fig. 3 displays 2D SAXS profiles of the unfractionated and the fractionated SI-2 as well as their circular averaged scattering intensity plot. The SAXS profiles of the two samples indicate that both block copolymers form a gyroid morphology as expected from their composition [5,38]. In Fig. 3(A), 2D SAXS image of the unfractionated sample displays a discrete diffraction pattern from the [220] plane while a continuous ring pattern from the [211] plane. Such speckle pattern indicative of the long-range ordering or large grain size has been reported previously by Hajduk et al. for a PS-*b*-PI system after transforming the lamellar phase to the gyroid phase by annealing [38]. In case of the fractionated sample, the speckle pattern becomes much more pronounced to show strong diffraction spots from both [211] and [220] planes as can be seen in Fig. 3(B). The circular average plots in Fig. 3(C) and (D) also show a clear difference between the two samples. The two diffraction peaks are much sharper and better developed in the fractionated sample. These results indicate that the fractionated sample has a long-range order, which corresponds to a larger grain size. Fig. 4 shows TEM images of the fractionated and unfractionated samples. A single grain double gyroid structure larger than $1 \times 1\ \mu m$ area was observed for the fractionated sample, while multi-grain structure is evident in the case of unfractionated one. These results also indicate clearly that the homogeneity of block copolymers leads to a larger grain size in the phase-segregated morphology.

3.4. Rheological behavior

We also investigated the effect of the fractionation on the order–order transition and order–disorder transition of the block copolymers [3,39–41]. SI-3 has a composition to exhibit various morphological changes upon heating. The phase transition

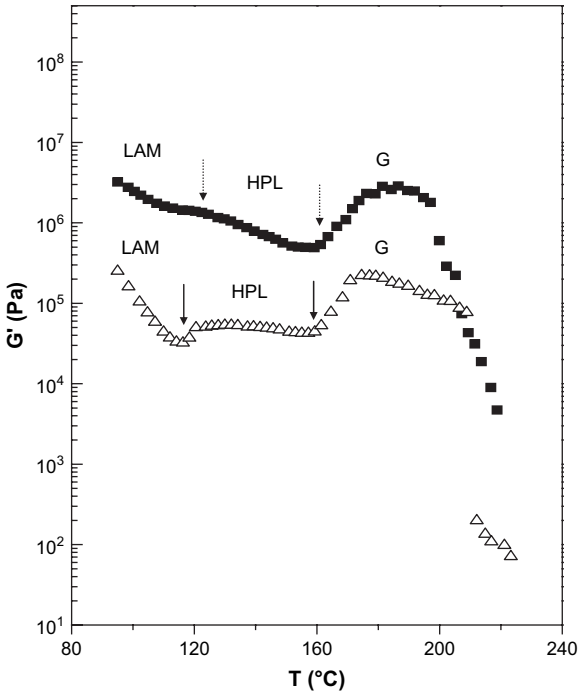

Fig. 5. Dynamic storage modulus (G') as a function of temperature for the unfractionated (■) and the fractionated (△) SI-3. Data of the unfractionated sample are vertically shifted by multiplying 100 for visual clarity. The fractionated sample exhibited morphological transitions more clearly than that of the unfractionated PS-*b*-PI. The arrows indicate the phase transition temperatures determined from the SAXS measurements [27].

behavior of block copolymers can be easily monitored by rheological measurements. Fig. 5 shows the change of the dynamic storage modulus as a function of temperature. Previously, we reported on the phase behavior of this sample by SAXS measurements [27]. The phase transition temperatures determined by rheological measurements are consistent with the SAXS results indicated with arrows. However, the fractionated sample exhibited much sharper morphological transitions than that of the unfractionated PS-*b*-PI.

In summary, the molecular weight distribution effect on the phase behavior of block copolymers was investigated using three PS-*b*-PI samples of different compositions. The PS-*b*-PI samples were prepared by anionic polymerization and the homo-PS precursors were removed. The purified PS-*b*-PI samples were further fractionated into the fractions of similar molecular weight and composition to the unfractionated PS-*b*-PI, but with much narrower distributions in both molecular weight and composition. These fractionated samples exhibited narrower interfacial thickness, larger grain size, and sharper morphological transitions comparing with the unfractionated PS-*b*-PI.

Acknowledgements

TC acknowledges the supports from KOSEF (National Research Laboratory and Center for Integrated Molecular Systems) and the BK21 program. JK acknowledges the support from KOSEF (National Creativity Research Initiative Center for Block Copolymer Self-Assembly). The XR and SAXS measurements at PAL were supported by the Ministry of Science and Technology and the POSCO.

References

[1] Hamley IW. The physics of block copolymers. New York: Oxford University Press; 1998.
[2] Park C, Yoon J, Thomas EL. Polymer 2003;44(22):6725.
[3] Leibler L. Marcromolecules 1980;13(6):1602.
[4] Bates FS, Schulz MF, Khandpur AK, Foerster S, Rosedale JH. Faraday Discuss 1994;98:7.
[5] Khandpur AK, Forster S, Bates FS, Hamley IW, Ryan AJ, Bras W, et al. Macromolecules 1995;28(26):8796.
[6] Thurn-Albrecht T, Schotter J, Kastle CA, Emley N, Shibauchi T, Krusin-Elbaum L, et al. Science 2000;290(5499):2126.
[7] Urbas A, Sharp R, Fink Y, Thomas EL, Xenidou M, Fetters LJ. Adv Mater 2000; 12(11):812.
[8] Black CT, Guarini KW, Milkove KR, Baker SM, Russell TP, Tuominen MT. Appl Phys Lett 2001;79(3):409.
[9] Cheng JY, Ross CA, Chan VZH, Thomas EL, Lammertink RGH, Vancso GJ. Adv Mater 2001;13(15):1174.
[10] Li X, Peng J, Wen Y, Kim DH, Knoll W. Polymer 2007;48(8):2434.
[11] Hsieh HL, Quirk RP. Anionic polymerization: principles and practical applications. New York: Marcel-Dekker; 1996.
[12] Lee W, Lee H, Cha J, Chang T, Hanley KJ, Lodge TP. Macromolecules 2000;33: 5111.
[13] von Werne TA, Germack DS, Hagberg EC, Sheares VV, Hawker CJ, Carter KR. J Am Chem Soc 2003;125(13):3831.
[14] Kowalewski T, McCullough RD, Matyjaszewski K. Eur Phys J E Soft Matter 2003;10(1):5.
[15] Schilli CM, Zhang M, Rizzardo E, Thang SH, Chong YK, Edwards K, et al. Macromolecules 2004;37(21):7861.
[16] Sides SW, Fredrickson GH. J Chem Phys 2004;121(10):4974.
[17] Cooke DM, Shi A-C. Macromolecules 2006;39(19):6661.
[18] Matsen MW. Eur Phys J E Soft Matter 2007;21(3):199.
[19] Hashimoto T, Tanaka H, Hasegawa H. Macromolecules 1985;18(10):1864.
[20] Noro A, Cho D, Takano A, Matsushita Y. Macromolecules 2005;38(10):4371.
[21] Lynd NA, Hillmyer MA. Macromolecules 2005;38(21):8803.
[22] Torikai N, Noro A, Okuda M, Odamaki F, Kawaguchi D, Takano A, et al. Physica B 2006;385–386:709.
[23] Meuler AJ, Ellison CJ, Evans CM, Hillmyer MA, Bates FS. Macromolecules 2007; 40(20):7072.
[24] Chang T. J Polym Sci Polym Phys Ed 2005;43(13):1591.
[25] Chang T. Adv Polym Sci 2003;163:1.
[26] Park S, Cho D, Ryu J, Kwon K, Lee W, Chang T. Macromolecules 2002;35(15): 5974.
[27] Park S, Kwon K, Cho D, Lee B, Ree M, Chang T. Macromolecules 2003;36(12): 4662.
[28] Park S, Park I, Chang T, Ryu C-Y. J Am Chem Soc 2004;126(29):8906.
[29] Im K, Park H-W, Kim Y, Chung B, Ree M, Chang T. Anal Chem 2007;79(3):1067.
[30] Lee W, Cho D, Chang T, Hanley KJ, Lodge TP. Macromolecules 2001;34(7):2353.
[31] Kwon K, Lee W, Cho D, Chang T. Korea Polym J 1999;7(5):321.
[32] Bolze J, Ree M, Youn HS, Chu S-H, Char K. Langmuir 2001;17(21):6683.
[33] Bolze J, Kim J, Huang JY, Rah S, Youn HS. Macromol Res 2002;10(1):2.
[34] Helfand E. Polym Sci Technol 1974;4:141.
[35] Kiessig H. Ann Phys 1931;10:769.
[36] Parratt LG. Phys Rev 1954;95:359.
[37] Russell TP. Mater Sci Rep 1990;5(4–5):171.
[38] Hajduk DA, Harper PE, Gruner SM, Honeker CC, Kim G, Thomas EL, et al. Macromolecules 1994;27(15):4063.
[39] Almdal K, Koppi KA, Bates FS, Mortensen K. Macromolecules 1992;25(6):1743.
[40] Matsen MW, Schick M. Macromolecules 1994;27(14):4014.
[41] Kim JK, Lee HH, Gu Q-J, Chang T, Jeong YH. Macromolecules 1998;31(12):4045.